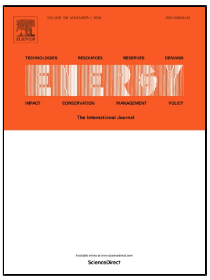

Experimental and analytic study of a Hybrid Solar/Biomass Rural Heating System

Xinghui Zhang, Jiaojiao Yang, Yi Fan, Xudong Zhao, Ruimiao Yan, Juan Zhao, Steve Myers

PII:	S0360-5442(19)32087-0
DOI:	https://doi.org/10.1016/j.energy.2019.116392
Reference:	EGY 116392
To appear in:	*Energy*
Received Date:	03 May 2019
Accepted Date:	17 October 2019

Please cite this article as: Xinghui Zhang, Jiaojiao Yang, Yi Fan, Xudong Zhao, Ruimiao Yan, Juan Zhao, Steve Myers, Experimental and analytic study of a Hybrid Solar/Biomass Rural Heating System, *Energy* (2019), https://doi.org/10.1016/j.energy.2019.116392

Experimental and analytic study of a Hybrid Solar/Biomass Rural Heating System

Xinghui Zhang[a], Jiaojiao Yang[a], Yi Fan[b], Xudong Zhao[a,b,*], Ruimiao Yan[a], Juan Zhao[c], Steve Myers[b]

[a] College of Environmental Science and Engineering, Taiyuan University of Technology, Taiyuan, Shanxi, P. R. China, 030024

[b]School of Engineering and Computer Science, University of Hull, Hull, United Kingdom, HU6 7RX

[c]School of Urban Plan and Municipal Engineering, Xi'an Polytechnic University, Xi'an, China, 710048

[*]Corresponding author: Prof. Xudong Zhao, Email: xudong.zhao@hull.ac.uk

Highlights

- The simulation and actual operation of solar/biomass heating system was undertaken.
- The thermal efficiency of solar thermal panels-array is around 65%.
- Ratios of solar and biomass energy usage are 63.31% and 36.69% respectively.
- The exergy efficiency of solar/biomass rural heating system is 16.17%.

Abstract: This paper presents a dedicated analytic and experimental study of a hybrid solar/biomass space heating system incorporating a micro-channel solar thermal panels-array, a biomass boiler and a dedicated control algorithm. This system enables the smart and joint use of solar and biomass energies to provide a comfortable indoor environment. The in-situ testing of the system was undertaken and the data obtained from the testing were analysed using Grubbs method to formulate the experimental thermal efficiency equation for the solar panels-array and the heat conversion factor equation for the combined heat storage/exchanging water tank. The annual energy performance of the hybrid system was investigated using a professional building energy simulation program (EnergyPlus), which can predict the heat load profile of house, the ratio of energy usage from solar/biomass sources and the primary energy/exergy efficiencies. The thermal

efficiency of the solar thermal panels-array is in the range of 60% to 70%. The heat storage water tank has a heat conversion factor in the range of 0.94 to 0.98. The heat load index per unit area is 46.86 W/m^2 and cumulative heating energy consumption with 100 m^2 house is 24.3 GJ during a heating season. The total annual energy demand of the solar/biomass heating system is around 35.91 GJ, of which the sun provides 63.31% and biomass provides 36.69%. The primary energy and exergy efficiencies of the solar/biomass rural heating system are 67.66% and 16.17% respectively. However, when the total input electrical exergy is traced back to its primary energy source, i.e. a coal-fired power plant, the exergy efficiency falls from 23.14% to 7.27%. Compared to the traditional primary energy supply system, the energy conversion effect and effective utilisation degree of the solar/biomass heating system are relatively higher.

Keywords: Solar energy; Biomass energy; Micro-channel panel; Rural house; EnergyPlus; Exergy efficiency

Nomenclature

A	The area of solar panels, m^2.
C_g	The specific heat capacity of glycol, kJ/(kg·°C).
Ex_{bio}	Chemical exergy provided by biomass solid fuel, GJ.
Ex_{coal}	Chemical exergy provided by the coal burning, GJ.
Ex_n	Income exergy, GJ.
Ex_{sun}	Solar absorption exergy, GJ.
F	Heat conversion factor of the heat storage/exchanging water tank.
G_{95}	The Grubbs threshold (confidence coefficient is 95%).
H	The height of water tank, mm.
ΔH	Chemical exergy of coal, MJ/kg.
ΔH_h	High heating value (HHV) of fuel, MJ/kg.
ΔH_l	Low heating value (LHV) of fuel, MJ/kg.
I	Solar radiation intensity, W/m^2.
Q	The heat from the heat source, W.
Q_l	The heat loss of insulation of water tank, W.

Q_2	Other heat loss of water tank, W.
Q_{bio}	Input energy from biomass energy, GJ.
Q_{loss}	The heat loss of the heat storage/exchanging water tank, W.
Q_n	The cumulative heating energy consumption of room within the heating period, GJ.
Q_s	The heat load of room, W.
Q_{sun}	Input energy from solar energy, GJ.
S	Heat storage capacity of the water tank, W.
T_a	The heating outdoor calculated absolute temperature of Lvliang, K.
T_n	Indoor design absolute temperature, K.
T_p	The average absolute temperature of microchannel, K.
V	Industrial waste gas discharge coefficient, m^3/t.
W	The electrical energy consumed by air source heat pump within the heating period, GJ.
d_1	The inside diameter of water tank, mm.
d_2	The outside diameter of water tank, mm.
H	Convection heat transfer coefficient between water tank and environment, 2.79 $W/(m^2 \cdot K)$.
m	Mass flow of glycol, kg/s.
R	Latent heat of water vaporization, 2.5 MJ/kg.
S	The standard deviation.
t_a	Ambient temperature, °C.
t_e	The indoor environment temperature, 10 ℃.
t_i	Inlet temperature of solar panels, °C.
t_o	Outlet temperature of solar panels, °C.
t_t	The hot water temperature of tank, ℃.
W	The mass fraction of water of biomass solid fuel, 1%~3%.

Greek symbols

Δ	The thickness of the insulation layer, mm.
H	Solar thermal efficiency, %.
η_Q	Primary energy efficiency of system, %.
η_{Ex}	Exergy efficiency of system, %.

λ	The thermal conductivity of polyurethane material, 0.023 W/(m·℃).

1. Introduction

Space heating in Northern China is a necessity but also a major source of pollution that has caused terrible haze and environment deterioration, due to a major reliance on the coal. This is particularly the case for rural houses[1]. Poor energy efficiency of the coal-fired boilers has created a huge amount of primary energy waste and provides inadequate indoor thermal comfort, which has caused severe health and safety problem for farmers[2, 3].

A survey has been conducted by the authors to inform the selection of alternative heating systems based on a case study of over 30 villages in Northern China[4]. A common terminal heating device used in Northern China, 'Kang', is used as a heated bed, but also acts as a heating tunnel to heat the whole of the house in rural areas. There are two types of 'Kang' that are currently in use; suspended and floor-based. The suspended type provides better energy efficiency and thus can achieve 30~50% saving in burning fuel and 5~6 ℃ higher indoor temperature compared to the floor-based type. However, the suspended Kang has a higher surface temperature that makes the occupier feel uncomfortable[5]. Bio-fuel is the preferred energy source as it is relatively eco-friendly when compared to traditional fossil fuels[6]. Bio-gas derived from collective livestock husbandries available within rural areas of Northern China is a regionally-available energy source[7]. However, the shortage of the raw materials (i.e. livestock husbandries) has greatly limited its scope of application[8]. Straw Gasification is another solution for generating bio-fuels that can be used to providing space heating and cooking for rural houses[9]. However, the operational cost of such a system is higher than the others, due to the necessity of a complex pipeline layout and potential toxic risk[10].

Solar energy is a long term renewable source that can be used for space heating. Overall the solar heating system has a wide range of applications on a global scale. In Europe, particularly Germany, solar power has been utilised within rural houses for heating, which has generated excellent energy savings and thermal comfort[11, 12]. In Africa, many countries made great efforts to utilize solar power within rural house heating. For example, Kenya has installed over 10 mega-watts of solar heating systems within around 320,000 rural households, which ranks as one of the largest markets

in the world[13]. China has been reckoned as the world largest market and technology provider in rural house solar heating owing to its vast territory, high demand for heating and advanced solar industry[14]. However, due to the intermittent and time-varying nature of solar radiation throughout the heating season, solar energy alone can't provide sustainable, stable and continuous heating services to rural houses. Hence alternative energy sources must be selected to work in conjunction with solar power[15].

A variety of energy sources are available for this purpose, such as gas, coal, electricity and bio-fuel[4, 16]. A gas boiler can be integrated into a solar heating system and provide match-up energy in addition to solar energy. However, there has been a bottleneck in the process of converting the fuel source from coal to gas. Traditional coal-fired boilers are a common solution to this service, but it will cause severe environmental pollution and poor indoor air quality[17]. Electrical heaters and heat pumps are available choices that can convert electrical energy into heat. The electrical heater, making use of the high-grade electrical energy to generate the secondary heat energy, is apparently energy inefficient. A heat pump can achieve higher energy efficiency due to the use of a mechanical vapor compression cycle and is therefore considered a better choice[18]. However, the high cost of a heat pump makes it difficult for farmers to invest. Bio-fuel is considered an ideal choice as the supplementary energy source for solar energy systems, as it is eco-friendly and promotes rural economies that produce biofuel crops[19].

Currently there is limited research available on the combined use of solar and biomass energies, due to a lack of knowledge and data relating to such systems. Liu[20] proposed two hybrid solar/biomass power generation systems, involving a solar thermal-chemical reaction and a thermal-to-power conversion respectively. The thermal-chemical cycle system provides a better performance with an overall energy efficiency of 28.03% whilst the solar-to-electric conversion efficiency of 18.49%. Eziyi[21] proposed a hybrid renewable energy system, comprising photovoltaic array, battery, and biomass-fueled generator with gasifier. The system utilizes multiple conversion devices which, when being integrated into a system, can mitigate the weakness of the individual devices under separate operational condition. Chasapis[22] presented the operational performance of a hybrid solar thermal-biomass space heating system which, built

in Greece and serving a 60 m^2 office block, achieved a solar energy ratio of 52.9% and biomass energy ratio of 47.1%. Boonrit [23] conducted the experimental study of the performance of a solar-biomass hybrid air-conditioning system at quasi-steady state conditions. The results indicate that the system was operating at around 75% of nominal capacity with an average system coefficient of performance (COP) of 0.11. Compared to the results derived from other studies, the system in study has a higher heating output and a higher COP.

With these limited results it is difficult to carry out a design and performance efficiency assessment of the hybrid solar/biomass heating system. In order to overcome the difficulties we conducted a dedicated investigation of such a system based on a typical rural house in Northern China, with on-site testing conducted in Lvliang city. The annual energy performance of the hybrid system was investigated and used to predict the heat load profile of the service house, the ratio of energy usage from solar/biomass sources and primary energy/exergy efficiencies of the system. Here we provide a feasible method for the design and performance assessment of a hybrid solar/biomass heating system (or similar), which contributes to fossil fuel energy saving and the reduction of polluting gas emissions.

2. System set-up and operational strategy

2.1 The system description

Figure 1 shows the schematic of the hybrid solar/biomass heating system and Figure 2 presents the experimental set-up. This system consists of two loops: heat generation/sourcing (first) and space heating (second), which are coupled by a combined heat exchanging/storage unit. This unit can receive the heat delivered from the solar panels-array, or the biomass boiler via the working fluid in the first loop, which is a glycol solution of 20% concentration and a freezing point of -9 ^oC. The heat received will be transferred to the second loop fluid (water) to provide space heating to the serviced room via the connected radiant heating coils in the floor. When the heat demand of the room space is less than the heat supply, indicated by a high fluid temperature in the second loop, the control system will transfer the excess heat into the storage unit. Conversely, when the heat demand of the room space is more than the heat supply, indicated by a low fluid temperature in the second loop, the control system will transfer the required amount of heat from the storage

unit into the fluid in the second loop. Within the first loop the solar panels-array and biomass boiler will be laid in parallel as shown in Figure 1, and hence will be brought into action alternatively to deliver a relatively stable heat supply to the room space. This joint operation will be achieved by a dedicated control system.

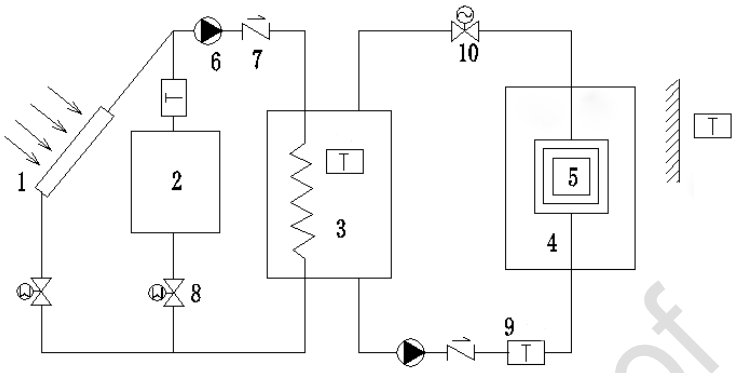

1. Solar panels 2. Biomass boiler 3. Heat storage/exchanging water tank
4. Rural house 5. Floor radiant heating coil 6. Water pump 7. Check valve
8. Solenoid valve 9. Temperature sensor 10. Electric control valve

Figure 1. The schematic diagram of solar/biomass heating system

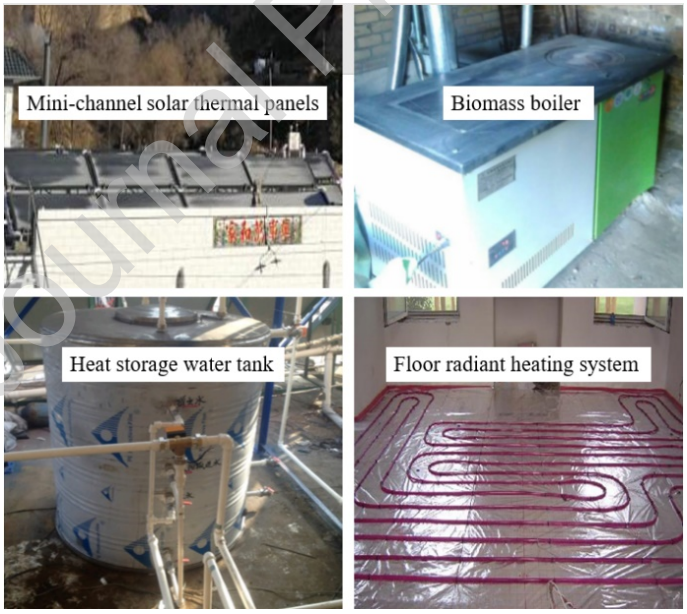

Figure 2. The solar/biomass heating experimental system set-up

A solar thermal panels-array is comprised of 10 individual series-connected panels, each having 1000 mm×2000 mm in size as shown schematically in Figure 2. When the solar thermal panels are mainly used for heating in winter, the optimal installation angle of the solar collectors can be

accurately calculated. The optimal installation angle for Lvliang city (N37°5' E111°08') is 37.3°. An individual panel, as shown in Figures 3 and 4, is comprised of several functional layers; (1) Professional glazed cover for the solar thermal panel to prevent heat loss and protect the thermal panel, (2) Air layer to provide a gap between the panel and glass thus reducing the heat loss to the surroundings, (3) Black chrome absorber layer to increase the absorptivity of the panel for solar irradiance, (4) Mini-channels layer (28 mm×5 mm) which has numerous mini-channel rectangular pipes and is connected to the head tubes on both ends, (5) Insulation layer to minimize the heat loss of the panel to the surroundings, and (6) Framework. The photograph of the panel is presented in Figure 5, whilst the sizes and material are presented in Table 1.

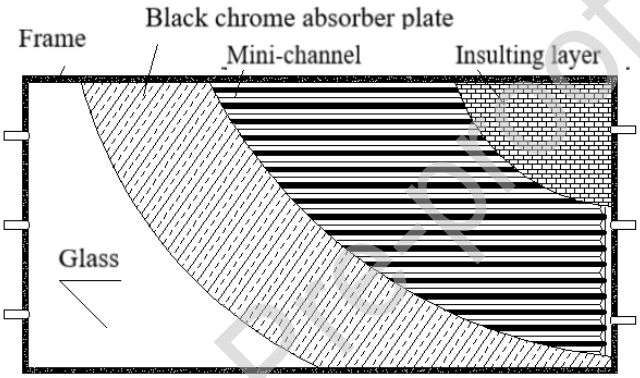

Figure 3. Front view of the mini-channel solar thermal panel

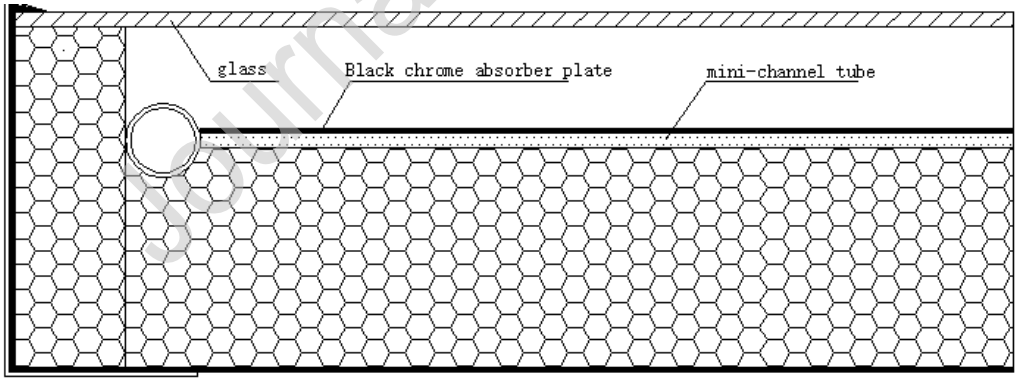

Figure 4. Sectional view of the mini-channel solar thermal panel

Figure 5. Photograph of the mini-channel solar thermal panel

Table 1. Sizes and materials of the mini-channel solar thermal panel

Number	Element	Thickness/mm	Function
1	Low iron tempered glass plate	3.2	Based panel; prevent dust and rain water
2	Air layer	0.1	Reduce heat loss to surroundings
3	Black chrome absorber plate	0.1	Enhance solar thermal efficiency
4	Mini-channel tube	4	The flow channel of refrigerant (glycol solution)
5	Phenolic plate	62	Thermal insulation layer
6	Frame	80	Packaging, fix, protection

A biomass boiler from Zhongke Bosheng (Beijing) Amperex Technology Limited was selected as the supplementary device to the solar panels-array. A photograph of the selected biomass boiler is presented in Figure 2, whilst its technical parameters are listed in Table 2. In this system the biomass boiler is in operation only when solar radiation is weak or unavailable. The technical advantages of biomass boiler are rapid ignition and heating, continuous feeding, the use of fully closed combustion technology and heat insulation. Figure 6 shows the biomass solid fuel and burning soot which can be used as fertilizer. The combustion value of biomass fuel is 4500 kcal/kg.

Table 2. Technical parameters of the biomass boiler

Name	Parameter	Name	Parameter
Type	DHS-C-1	Size	1000 mm×500 mm×700 mm
Rated thermal efficiency (LHV)	85%	Bin capacity	50 kg
Heating power	8~12 kW	Heating area	60~120 m^2
Electric power	98 W	Fuel consumption	1.5~3 kg/h

(a) Biomass solid fuel (b) Burning soot

Figure 6. The biomass solid fuel and burning soot

A compact heat storage/exchanging water tank is used in this project. There are four main functional parts incorporated into the tank; (1) Heat exchange water tank at the top of the outer heat storage/exchanging water tank, (2) Heat storage tank containing 1m^3 of water and a submerged water pump, which is used to store heat in the tank water when the solar irradiation is high and release heat to the room space when the solar irradiation is low, (3) Coil-type-heat-exchanger embedded into the bottom of the heat storage/exchanging water tank and connected to the biomass boiler to supply auxiliary heat for the system and (4) a hot water supply part merged into the bottom of water tank with a coil-type-heat-exchanger. The photograph of water tank is shown in Figure 2 and its technical data are listed in Table 3.

Table 3. Technical data of the heat storage/exchanging water tank

Name	*H*/mm	Diameter/mm	*δ*/mm	Insulation material	Volume/m^3
Dimension	1180	1190	50	Polyurethane	1

2.2 Operational strategy

Solar heating systems are currently designed to compare the solar panel temperature and the upper/lower limit temperature set by the water tank in order to control the solar heating system. For example, when the outdoor temperature rises, the controller can reduce the water supply temperature to adapt to the room heat load changes. Here we improve the control system to maximize the solar energy efficiency with the flexible use of a solar collector, biomass boiler and water tank. The centralized control system reduces the water supply temperature as the outdoor temperature increases by varying the water flow in steps, which can extend the heating time of the solar energy collected.

2.2.1 Heat generation/sourcing (first) loop

When the water temperature in the tank is greater than the required water supply temperature and less than the fluid temperature at the solar panels outlet, then part of the heat from the solar panels is transferred to the second water loop water for the use of space heating and the remaining heat is stored in the tank. When both the fluid temperature at the solar panels outlet and the water

temperature in the tank are less than the required water supply temperature, the solar panels are switched off and biomass boiler is switched on. When the fluid temperature at the solar panels outlet is greater than the supply water temperature, the biomass boiler is switched off and the solar panels are switched on.

2.2.2 Heat storage/exchanging water tank

When the water temperature in the tank (i.e., heat storage/exchanging unit) is greater than the supply water temperature and the fluid temperature at the solar panels outlet, then the control system is activated to allow the heat storage unit to deliver heat to the room space.

2.2.3 Space heating (second) loop

A step control approach is applied to meet the balance between the heat demand of the room space and the heat supply from the solar loop and heat storage/exchanging water tank. This means that the flow rate of the water in the heating loop will be adjusted in steps to match the variation of the ambient temperature. For our system the ambient temperature range determines the mode of operation for the heat pump as follows; -12.6 °C to -5 °C the pump operates at 100%, -5 °C to 0 °C the pump is adjusted to 80% and 0 °C to 10 °C the pump is adjusted to 60%. When the indoor air temperature is greater than 18 ℃ the heat supply to the service room is terminated by switching off the water circulation pump in the heating loop. In this case, the heat from the solar panels is stored in the water tank. When the indoor air temperature is less than 16 ℃, the water pump is switched on to resume heating of the service room.

3. Experimental testing and results analysis

Due to limited time and resource it is not currently feasible to run a full winter test of the system. Instead, a short-term test was carried out in order to assess the performance of the solar panels-array and heat storage/exchanging unit. This involves the development of the correlations between the solar thermal efficiency of the solar panels-array, the heat conversion factor of the heat storage/exchanging tank and their relevant operational conditions. When these two critical correlations are established the annual energy performance of the hybrid solar/biomass system can thus be estimated by EnergyPlus.

3.1 Testing instrument and procedure

The above system was equipped with various measurement instruments and sensors. The temperature, flow rate and pressure of the fluid in the solar and heating loops were measured using the platinum resistance thermometer probes, flow meters and pressure gauges, respectively, which were appropriately installed into the system. The output signals of all the measurement instruments installed in the system were transmitted to a Keysight 34970A Data Logger and then to a computer. The specification, quantity, and installation point of the sensors/meters are outlined in Table 4. The tests were carried out under real-time operational condition in a typical rural house in Lvliang City China, over 3 days (i.e. 14th to 16th December 2017), see Figures 7, 8 and 9.

Table 4. List of the testing and monitoring devices

Devices	Type	Range Accuracy	Output signal	Quantity	Location
Pyranometer	JZ-TQB-2C	0~2000 W/m^2	0~20 mV	1	Top of the collector
Flowmeter	MK-LWGY-DN25	1~10 m^3/h	4~20 mA	1	solar thermal panels entrance
Anemometer	HS-FS01(HuaKong)	0~30 m/s	4~20 mA	1	Top of the collector
Pressure gauge	YN60(JiangYin)	0~0.6 MPa		6	Inlet/outlet of water pump, solar thermal panels and water tank
Thermometer	PT1000(ZhongJia)			20	solar thermal panels; testing room; water tank; ambient, etc.

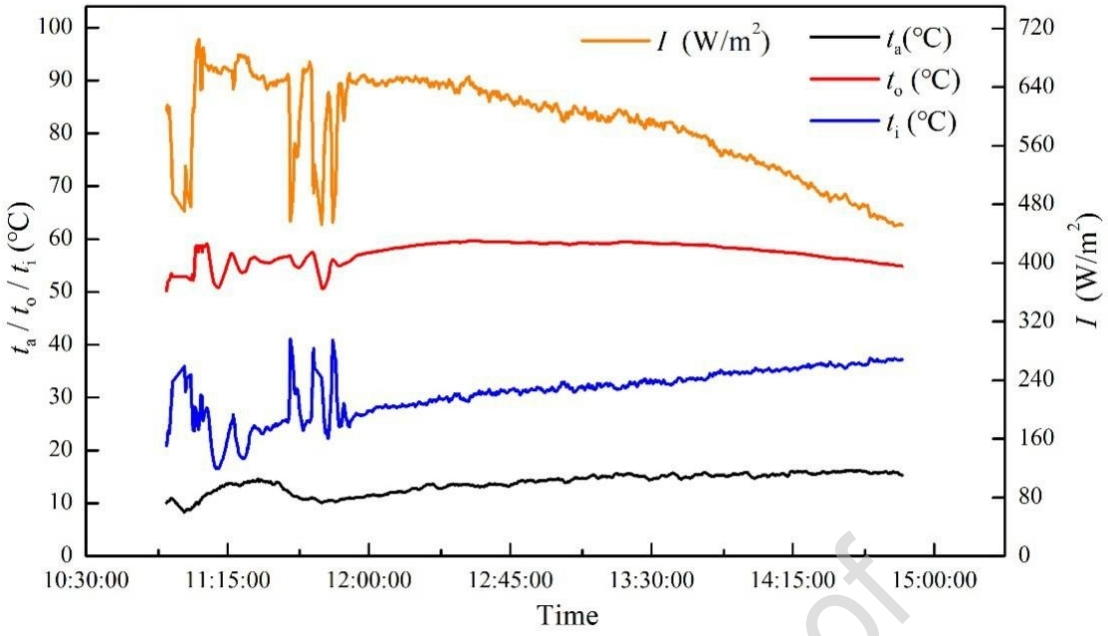

Figure 7. Experimental test data on 14th December 2017

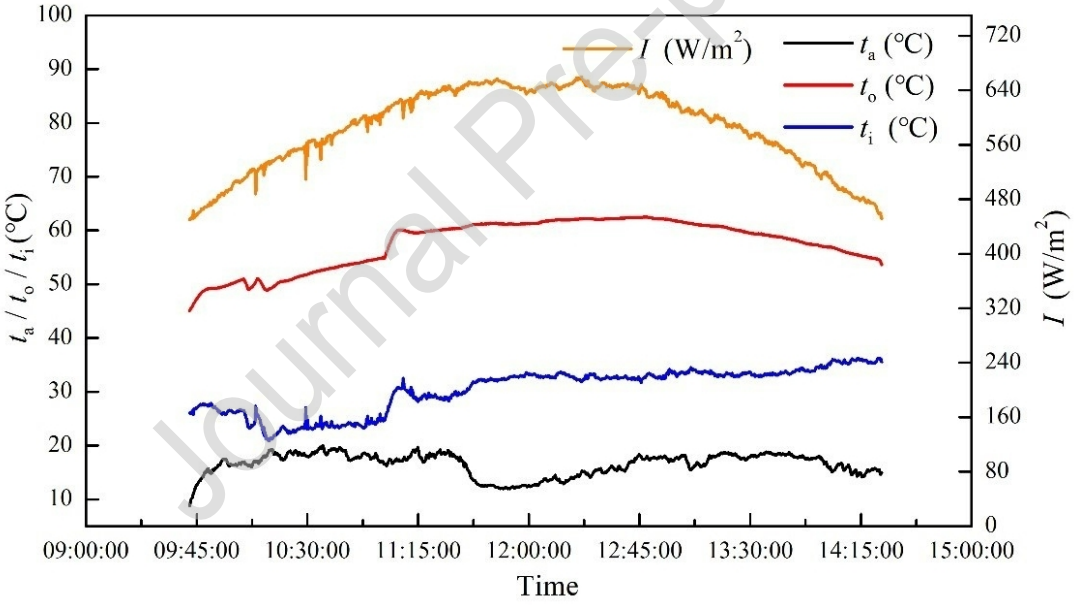

Figure 8. Experimental test data on 15th December 2017

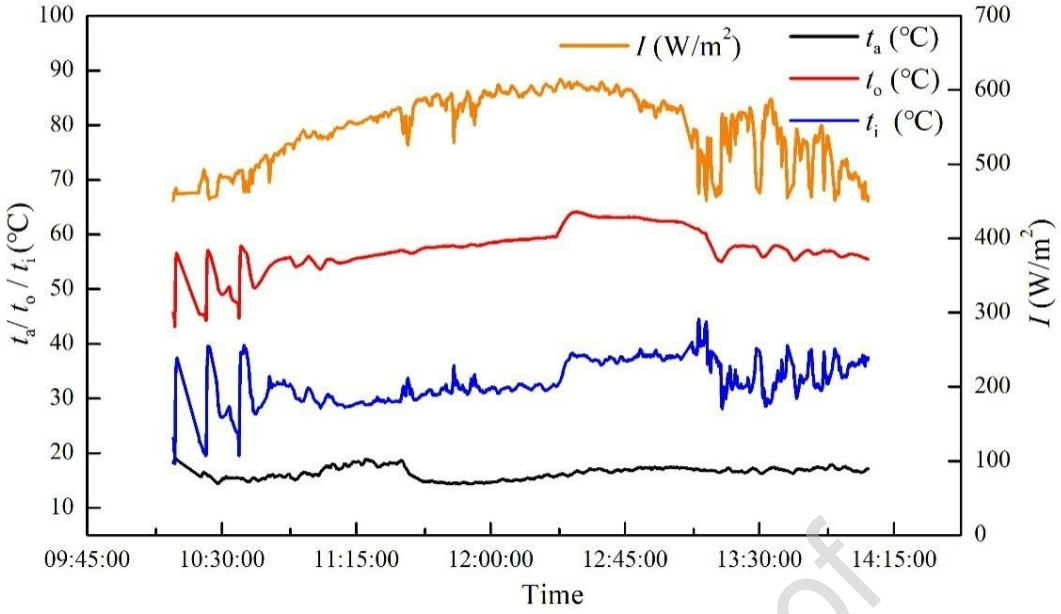

Figure 9. Experimental test data on 16th December 2017

Where, t_a is ambient temperature, °C. t_o is outlet temperature of solar panels, °C. t_i is inlet temperature of solar panels, °C, and I is solar radiation intensity, W/m^2.

3.2 Results analysis

3.2.1 Solar thermal efficiency of the hybrid solar/biomass heating system

With the measurement data obtained above in Figures 7, 8 and 9 the solar thermal efficiency was calculated using Equation 1 [24]. It should be noted that the working fluid of the solar loop is a mixture of 20% glycol and 80% water. At 40 ℃, which is the average temperature of the fluid at the inlet and outlet for the solar panels, the glycol solution has a density of 1021.83 kg/m^3, and specific heat capacity of 3.861 kJ/(kg·℃). The volume flow of glycol was measured as 0.082 cm^3/s.

$$\eta = \frac{C_g m(t_o - t_i)}{AI} \tag{1}$$

Where m is mass flow of glycol, kg/s. There is a certain deviation between the measured and the true value, due to systematic and random errors. This is due to the influence of experimental devices, environmental factors, testing methods and changes in measured objects. Therefore, according to Equation 1, the measurement data within 3 days are converted into η and $\frac{t_i - t_a}{I}$ for

statistical processing of data analysis, i.e., the selection of outlying data. The total number of data points is 4,317 after conversion. The Grubbs test method was adopted here to make the selection of outlying data, see Equation 2 [25] and Table 5. If G_i is greater than G_{95} obtained from the Grubbs critical values table, the corresponding data will be discarded[25].

$$G_i = \frac{\left|\eta_i - \bar{\eta}\right|}{s} \tag{2}$$

Table 5. Statistical processing of data analysis

$\frac{t_i - t_a}{I}$ Data segment	Total amount	s	$\bar{\eta}$	G_{95}	Removal amount	Remaining amount
0.00~0.02	85	0.0331	0.8085	3.151	19	66
0.02~0.04	674	0.0348	0.7232	3.754	105	569
0.04~0.06	2727	0.0286	0.6516	3.754	436	2291
0.06~0.08	592	0.0345	0.5617	3.754	108	484
0.08~0.10	98	0.0266	0.4923	3.201	31	67
0.10~0.12	87	0.0284	0.3709	3.160	14	73
0.12~0.14	54	0.0206	0.2741	2.986	12	42

The remaining number of data points is 3,592 after processing with the Grubbs test method. The relationship between η and $\frac{t_i - t_a}{I}$ was established for the remaining data points according to the least squares method, see Figure 10. The results show that the solar thermal efficiency has an inverse linear relationship with $\frac{t_i - t_a}{I}$, with an interception efficiency of 86.8% and slope gradient of -4.4871, see Equation 3.

$$\eta = 0.868 - 4.8671\frac{t_i - t_a}{I} \tag{3}$$

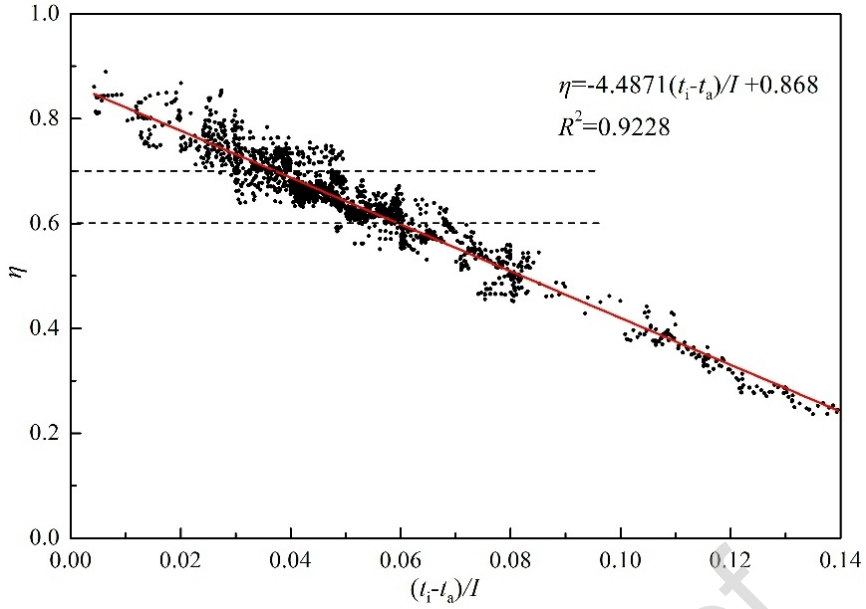

Figure 10. Correlation between η and $\frac{t_i - t_a}{I}$

According to Equation 1 the thermal efficiency of the solar thermal panels-array is mainly concentrated within the range of 60%~70%, which accounts for 68.3% of the remaining data, see Figure 10. Under the same condition, i.e., same heat consumption, solar energy guarantee rate, annual average daily solar radiation, and system loss, a higher average thermal efficiency of solar collectors leads to the reduced area of the solar collectors and thus reduced initial investment. As the thermal efficiency of the solar thermal panels-array is higher than common collectors, the investment cost of solar collectors can be reduced in the proposed system, which is the advantage of mini-channel solar thermal panel.

3.2.2 The heat conversion factor of the combined heat storage/exchanging water tank

The heat balance existing in the heat storage/exchanging water tank is shown in Equation 4 [26]. On this basis, the heat conversion factor of the combined heat storage/exchanging water tank (F) can be expressed by Equation 5 [26].

$$Q=Q_s+Q_{loss}+S \tag{4}$$

$$F=\frac{Q_s+S}{Q}=1-\frac{Q_{loss}}{Q} \tag{5}$$

The technical specifications of the heat storage/exchanging water tank are presented in Table 3. The heat loss of the heat storage/exchanging water tank (Q_{loss}) can be split into two parts; The heat loss through the enclosure of the tank, designated as Q_1, and the heat loss caused by air convection, water evaporation etc., designated as Q_2. By using conventional heat conduction and convection theory, Q_1 is calculated by using Equations 6 and 7 [26].

$$Q_1 = \frac{H(t_t - t_e)}{\frac{1}{2\pi\lambda}\ln\frac{d_2}{d_1} + \frac{1}{h\pi d_2}} + \frac{\frac{\pi}{2}d_1^2(t_t - t_e)}{\frac{\delta}{\lambda} + \frac{1}{h}} = 2.763(t_t - 10) \quad (6)$$

$$h = Nu\frac{\lambda}{H} = 0.1(Gr \cdot Pr)^{\frac{1}{3}}\frac{\lambda}{H} \quad (7)$$

The other heat loss (Q_2) represents the heat loss caused by air-to-water heat transfer, water evaporation, and other unexpected heat leakage. For simplicity, Q_2 is usually considered to be 50% of the enclosure heat loss (Q_1), and thus, the total heat loss is $1.5Q_1$, see Equation 8 [26].

$$Q_{loss} = Q_1 + Q_2 = 1.5Q_1 \quad (8)$$

On the basis of the above analysis, the relationship between the heat conversion factor (*F*) and $\frac{t_t - 10}{t_o - t_i}$ can be expressed as shown in Equation 9.

$$F = 1 - \frac{Q_{loss}}{C_g m(t_o - t_i)} = 1 - \frac{4.144(t_t - 10)}{323.51(t_o - t_i)} = 1 - 0.0128\frac{t_t - 10}{t_o - t_i} \quad (9)$$

4. Energy performance of the system

4.1 Rural residential house model

We address a typical rural residential house 14 m in length, 7 m in width, and 4 m in height and a floor area of around 100 m^2. The front façade of the house is facing southward. In order to investigate the thermal performance, annual load and energy consumption of the rural residence, a rural residential house model was established based on the plug-in OpenStudio of SketchUp, as shown in Figure 11. The heat transfer coefficients of the building envelopes are presented in Table

6, measured using a BES-GP intelligent multi-channel temperature/heat flow detector. Thermal properties of the building components used in the modelling are same as the actual figures of the rural house, thus providing a true reflection of the heat load in real life conditions.

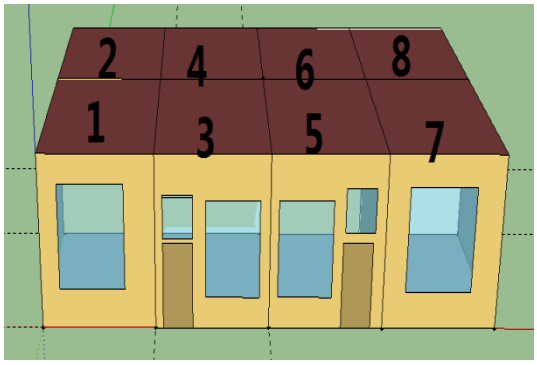

Figure 11. Schematic diagram of the rural residence

Table 6. Heat transfer coefficients of the building envelopes

Part	Structure	Dimension/m	K [W/(m²·℃)]
Wall	370 mm brick wall Plastering + 50 mm extruded polystyrene board	—	0.47
External doors	Pine wood door	0.9×1.8	2.9
Window	3 mm common glass aluminum alloy window frame (two layer)	1.5×1.8	1.54
Roof	Cement mortar + Insulation layer + Waterproof layer + Tile	14×7	0.37

4.2 Heating system model

The heating system model was established to investigate the energy collection and supply performance when serving a typical rural house. A low-temperature floor radiant heat supply loop and a combined solar panels/biomass heat collection loop are the major factors of this model. Using IDF-Editor software we add the floor radiant heating system module and the solar/biomass energy collection module. This involves the code and integration of the equations for solar thermal efficiency, biomass boiler equation, and heat conversion factor into the computer programme established in the IDF-Editor software. This forms a comprehensive heat system model that can be used to assess the energy performance of the system.

4.3 Heating load profile of the service house

Both the heat balance and the modular system simulation methods are applied in EnergyPlus to calculate the annual load and energy consumption of the rural house[27]. The heat load period is from November 1 to March 31. The solar radiation intensity and outdoor dry bulb temperature of Lvliang city China (N37°5' E111°08') are shown in Figure 12. The annual heat load diagram is shown in Figure 13. The rural house has a floor area of 100 m^2, which has a calculated design heat load of 4.686 kW, the heat load index per unit area of 46.86 W/m^2 and cumulative heating energy consumption of 24.3 GJ (Q_n) during a heating season.

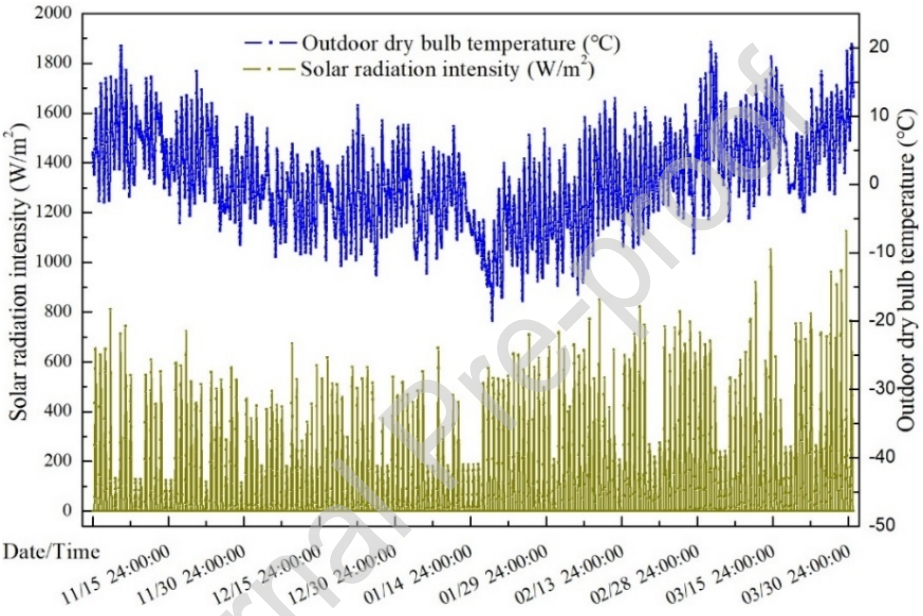

Figure 12. The solar radiation intensity and outdoor dry bulb temperature

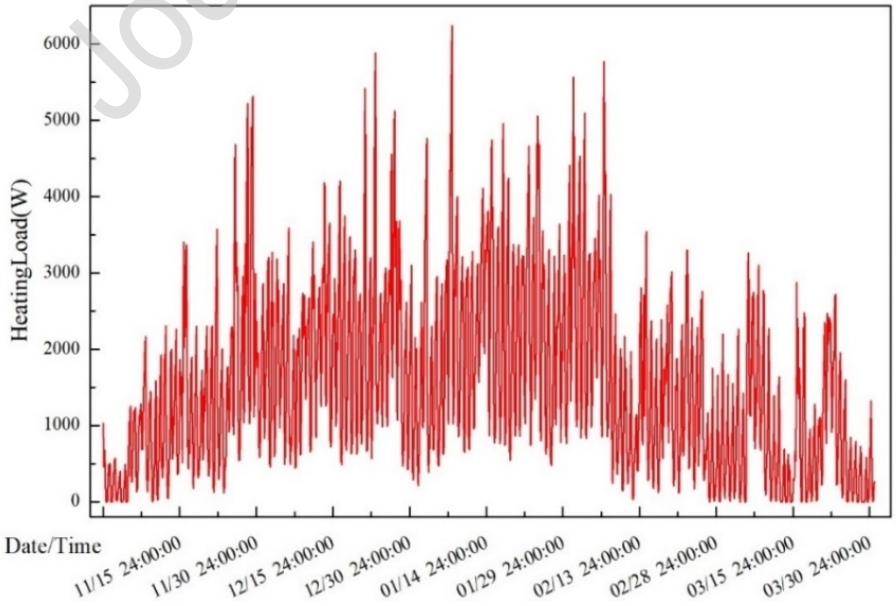

Figure 13. Annual heat load diagram

4.4 Annual energy supply and operational hour of the heating system

The heating load and time distribution of solar panels and biomass boiler are shown in Figure 14. The total input energy from both solar and biomass energy amounts to 35.92 GJ based on the data shown in Figure 14, including 22.74 GJ (Q_{sun}) from solar energy and 13.18 GJ (Q_{bio}) from biomass energy, which means the solar energy utilization rate is 63.31%, while the biomass energy utilization rate is 36.69%. The operational hours of solar panels and biomass boiler are 1,186 h and 1,239 h respectively. When neither the solar system or biomass boiler are operating, the heat storage/exchanging water tank plays its role in delivering heat to the room space, for around 749 h per annum. To summarize, the total heating hours of the service room is 1,975 h while the shutdown time of the heating system is 450 h.

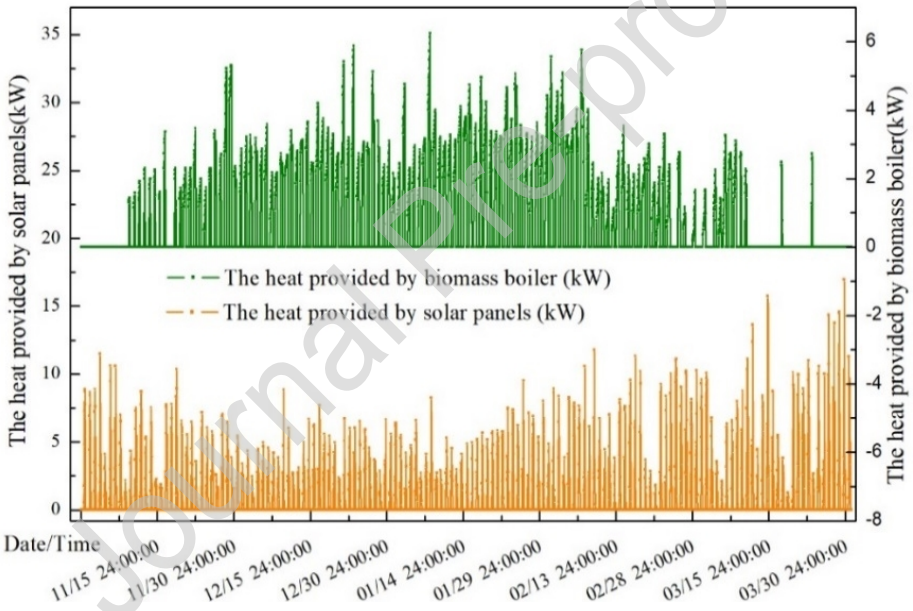

Figure 14. The heating load and time distribution of solar panels and biomass boiler

It is expected that the system has a service life time of 15 years, while the solid biomass fuel has a market price of 600 RMB/t. A calculation made by the authors indicates that the actual consumption of biomass fuel is 0.8 t during a heating season. In this case, the initial investment of the solar/biomass heating system is 16,000 RMB, including 7,000 RMB for solar panels, 4,500 RMB for the biomass boiler, 500RMB for the water tank, and 4,000 RMB for others. During the whole life cycle, the cost of biomass fuel is 7,200 RMB, leading to 7,000 RMB of solar system investment and 11,700RMB of biomass system investment, with investment ratios of 30.2% and

50.4% respectively.

4.5 Primary energy and exergy efficiencies

Exergy refers to the useful work of a given energy, which is also known as effective energy. Exergy, as a parameter for assessing the value of energy, defines the value of energy in terms of quantity and quality. Energy efficiency can only reflect energy difference in quantity and cannot fully reflect the real sense of energy utilization. Exergy efficiency can be introduced to consider both quantity and quality in energy balance. Match of the quality of energy between the demand and supply enables a rational utilisation of exergy, and this, improves the exergy efficiency.

During the heating season, the total input exergy of the solar/biomass heating system includes solar absorption exergy and chemical exergy provided by biomass solid fuel, and the income exergy is the heat exergy of the accumulated total load of the rural room. The formulas to calculate the primary energy and exergy efficiencies of the system are shown in Equations 10 and 11[28]. For an air source heat pump heating system, assuming a COP of 2.5 in the north for winter heating, the total input exergy is the electric exergy consumed by the air source heat pump and the income exergy is the heat exergy of the accumulated total load of the rural room. The formulas to calculate the primary energy and exergy efficiencies of the system are shown in Equations 12 and 13 [28]. If it is taken into account that the electric of the air source heat pump comes from a coal-fired power plant, then the total input exergy is the chemical exergy provided from burning coal, and the income exergy is the heat exergy of the accumulated total load of rural room. The calculation formulas of exergy efficiency is shown in Equation 14 [28].

$$\eta_Q = \frac{Q_{\mathrm{n}}}{Q_{\mathrm{sun}} + Q_{\mathrm{bio}}} \tag{10}$$

$$\eta_{Ex} = \frac{Ex_{\mathrm{n}}}{Ex_{\mathrm{sun}} + Ex_{\mathrm{bio}}} = \frac{Q_{\mathrm{n}}\left(1 - \frac{T_{\mathrm{a}}}{T_{\mathrm{n}}}\right)}{Q_{\mathrm{sun}}\left(1 - \frac{T_{\mathrm{a}}}{T_{\mathrm{p}}}\right) + \frac{\Delta H_{\mathrm{l}} + rw}{\Delta H_{\mathrm{h}}} Q_{\mathrm{bio}}} \tag{11}$$

$$\eta_Q^{'} = 30\% \frac{Q_{\mathrm{n}}}{W} \tag{12}$$

$$\eta_{Ex}' = \frac{Ex_{\mathrm{n}}}{W} = \frac{Q_{\mathrm{n}}(1-\frac{T_{\mathrm{a}}}{T_{\mathrm{n}}})}{\frac{65\%Q_{\mathrm{sun}}+85\%Q_{\mathrm{bio}}}{2.6}} \tag{13}$$

$$\eta_{Ex}'' = \frac{Ex_{\mathrm{n}}}{Ex_{\mathrm{coal}}} = \frac{Q_{\mathrm{n}}(1-\frac{T_{\mathrm{a}}}{T_{\mathrm{n}}})}{\frac{W}{30\%\Delta H_{\mathrm{h}}}\Delta H} \tag{14}$$

Where, η_Q is primary energy efficiency of solar/biomass system, %. η_Q' is primary energy efficiency of heat pump, %. Q_{n} is the cumulative heating energy consumption of room within the heating period, GJ. Q_{sun} is input energy from solar energy, GJ. Q_{bio} is input energy from biomass energy, GJ. η_{Ex} is exergy efficiency of solar/biomass system, %. η_{Ex}' is exergy efficiency of heat pump (electric exergy), %. η_{Ex}'' is exergy efficiency of heat pump (chemical exergy), %. Ex_{n} is income exergy, GJ. Ex_{sun} is solar absorption exergy, GJ. Ex_{bio} is chemical exergy provided by biomass solid fuel, GJ. Ex_{coal} is chemical exergy provided by the coal burning, GJ. T_{a} is the heating outdoor calculated absolute temperature of Lvliang, K. T_{n} is indoor design absolute temperature, K. T_{p} is the average absolute temperature of microchannel, K. ΔH_{l} is low heating value of fuel, MJ/kg. ΔH_{h} is high heating value of fuel, MJ/kg. ΔH is chemical exergy of coal, MJ/kg. W is the electrical energy consumed by air source heat pump within the heating period, GJ. r is latent heat of water vaporization, 2.5 MJ/kg. w is the mass fraction of water of biomass solid fuel, 1%~3%.

The calculated outdoor temperature for heating in Lvliang is -12.6 ℃, while the indoor design temperature for heating is 16 ℃ according to *the technical guidelines for rural housing energy conservation in severe cold and cold regions*, and the average temperature of microchannel is 45 ℃, i.e., the T_{a} is 260.4 K, T_{n} is 289 K, and T_{p} is 318 K. Q_{n} is 24.3 GJ， Q_{sun} is 22.74 GJ, and Q_{bio} is 13.18 GJ. The HHV and LHV of biomass solid fuel are 20.16 MJ/kg and 16.38 MJ/kg respectively, with carbon content of 75%~85%. The power generation efficiency of coal-fired power plants is set at 30%[28]. The high heating value of coal is set at 32.22 MJ/kg, and the chemical exergy of coal is set at 30.77 MJ/kg[29]. The primary energy and exergy efficiencies of the system are calculated according to the above relevant data and Eqs. (10)~(14), as shown in Table 7.

Table 7. Primary energy and exergy efficiencies of the systems

Name	Solar/biomass	Heat pump (electric exergy)	Heat pump (chemical exergy)
η_Q	67.66%	70.15%	70.15%
η_{Ex}	16.17%	23.14%	7.27%

Table 7 shows that the primary energy and exergy efficiencies of the solar/biomass heating system are 67.66% and 16.17% respectively. The primary energy and exergy efficiencies of the air source heat pump heating system are 70.15% and 23.14% respectively. However, when the total input electrical exergy is traced back to its primary energy source, namely a coal-fired power plant, then the exergy efficiency falls from 23.14% to 7.27%. Compared to the traditional primary energy supply system, the solar/biomass heating system has the advantage of high primary energy utilization and an improved exergy efficiency. The energy conversion effect and effective utilization degree of the solar/biomass heating system are higher than that for a heat pump (chemical exergy). Further, the solar/biomass heating system can achieve a good match in quality of energy between the supply and demand.

5. Conclusions

This paper presents an experimental and analytic study of a hybrid solar/biomass-driven rural house space heating system. This involves: (1) experimental testing of the system and characterization of the performance of the micro-channel solar panels-array and heat storage/exchanging water tank, by using Grubbs method, (2) annual energy performance analysis of the system by using EnergyPlus and the Plug-in OpenStudio of Sketchup; and (3) the primary energy and exergy efficiency analyses of the system.

It was found that the solar panels-array presented a good solar collection performance with an initial efficiency of 86.8% and a gradient slope of -4.8671. The thermal efficiencies of solar thermal panels-array are mainly concentrated in the range of 60%~70%. The heat storage water tank has a heat conversion factor in the range of 0.94~0.98. The heat load index per unit area is 46.86 W/m^2 and cumulative heating energy consumption with 100 m^2 house is 24.3 GJ during the

heating period. The total annual energy demand of the solar/biomass heating system is around 35.91 GJ; 22.74 GJ (63.31%) from the solar panels-array and 13.18 GJ (36.69%) from the biomass boile. Meanwhile, the primary energy and exergy efficiencies of the solar/biomass heating system are 67.66% and 16.17% respectively. The primary energy and exergy efficiencies of the air source heat pump heating system are 70.15% and 23.14% respectively. However, when the total input electrical exergy is traced back to its primary energy source, i.e. a coal-fired power plant, the exergy efficiency falls from 23.14% to 7.27%. Compared to the traditional primary energy supply system, the energy conversion effect and effective utilization degree of solar/biomass heating system are higher. Therefore, the hybrid solar/biomass heating system can be efficiently applied to warming rural houses and helps reducing the fossil fuel consumption and pollutant gas emissions.

References

[1] L. Perez-Lombard, J. Ortiz, I. R. Maestre. The map of energy flow in HVAC systems[J]. Applied Energy, 2011, 88 (12): 5020-5031.

[2] Meredydd Evans, Sha Yu, Bo Song, et al. Building energy efficiency in rural China[J]. Energy Policy, 2014, 64 (1): 243-251.

[3] Ming Shan, Pengsu Wang, Jiarong Li, et al. Energy and environment in Chinese rural buildings: Situations, challenges, and intervention strategies[J]. Building & Environment, 2015, 91: 271-282.

[4] Xinghui Zhang, Jiaojiao Yang, Xudong Zhao. Optimal study of the rural house space heating systems employing the AHP and FCE methods[J]. Energy, 2018, 150: 631-641.

[5] Zhiqiang John Zhai, Andrew Porter Yates, Duanmu Lin, et al. An evaluation and model of the Chinese Kang system to improve indoor thermal comfort in northeast rural China – Part-2: Result analysis[J]. Renewable Energy, 2015, 84 (6): 12-21.

[6] H.B. Goyal, Diptendu Seal, R.C. Saxena. Bio-fuels from thermochemical conversion of renewable resources: A review[J]. Renewable and Sustainable Energy Reviews, 2008, 12 (2): 504-517.

[7] Fei Li, Shengkui Cheng, Huilu Yu, et al. Waste from livestock and poultry breeding and its potential assessment of biogas energy in rural China[J]. Journal of Cleaner Production, 2016, 126 (126): 451-460.

[8] Peter Weiland. Biogas production: current state and perspectives[J]. Applied Microbiology and Biotechnology, 2010, 85 (4): 849.

[9] Bai Ming Chen, An Ning Chen, Zheng Feng Zhang, et al. Analysis on the Driving and Constraint Factors of Crop Straw Gasification and Commercialization Development[J]. Journal of Natural Resources, 2007, 259 (259): 59-68.

[10] Guang Qiao Cao, Zong Yi Zhang. Externality,influence factors and development countermeasures for straw gasification system for gas supply[J]. Renewable Energy Resources, 2008.

[11] Wood Janet. Solar energy in Germany: A Market Review[J]. Refocus, 2006, 7(3):24-30.

[12] F. J. Friedrich, H. Klein. Status of solar energy projects in the Federal Republic of Germany[J]. Harvard

Theological Review, 1977, 82 (5): 342-350.
[13] Janosch Ondraczek. The Sun Rises in the East (of Africa): A Comparison of the Development and Status of the Solar Energy Markets in Kenya and Tanzania[J]. Energy Policy, 2013, 56 (2): 407-417.
[14] Dahai Zhang, Jiaqi Wang, Yonggang Lin, et al. Present situation and future prospect of renewable energy in China[J]. Renewable & Sustainable Energy Reviews, 2017, 76: 865-871.
[15] Min Wang, Yanfeng Liu, Dengjia Wang, et al. Suitability analysis of auxiliary heat sources for solar heating in rural areas of Northwest China[J]. Heating Ventilating & Air Conditioning, 2018.
[16] Kai Zhang. Selection and discussion of auxiliary heat source of solar heating system[J]. Heating and cooling, 2012, (7): 46-48.
[17] Yan Rong, Zhu Haijing, Zheng Chuguang, et al. Emissions of organic hazardous air pollutants during Chinese coal combustion[J]. Energy, 2002, 27(5):485-503.
[18] H. E. Fang-Bing, W. U. Li-Jun, Wen Ping Wang. Design and Application of Solar Energy Hot Water System with Air Source Heat Pump and Gas Boiler[J]. Applied Energy Technology, 2014.
[19] M. F. Demirbas, Mustafa Balat. Recent advances on the production and utilization trends of bio-fuels: A global perspective[J]. Energy Conversion & Management, 2006, 47 (15): 2371-2381.
[20] Qibin Liu, Zhang Bai, Xiaohe Wang, et al. Investigation of thermodynamic performances for two solar-biomass hybrid combined cycle power generation systems[J]. Energy Conversion & Management, 2016, 122: 252-262.
[21] Ifegwu Eziyi, Anjaneyulu Krothapalli. Sustainable Rural Development: Solar/Biomass Hybrid Renewable Energy System[J]. Energy Procedia, 2014, 57: 1492-1501.
[22] D. Chasapis, V. Drosou, I. Papamechael, et al. Monitoring and operational results of a hybrid solar-biomass heating system[J]. Renewable Energy, 2008, 33 (8): 1759-1767.
[23] Boonrit Prasartkaew, S. Kumar. Experimental study on the performance of a solar-biomass hybrid air-conditioning system[J]. Renewable Energy, 2013, 57: 86-93.
[24] Zhangyuan Wang, Wansheng Yang, Feng Qiu, et al. Solar water heating: From theory, application, marketing and research[J]. Renewable & Sustainable Energy Reviews, 2015, 41 (41): 68-84.
[25] Hongchao Han. Gross Error Detection and Elimination of Subsidence Monitoring Data Based on Grubbs Test Method[J]. Bulletin of Surveying and Mapping, 2018.
[26] Huishu Yu, Chunlin Lu, Sumin Jin. Analysis of heat loss on heat storage water tank applied to heat pump Water Heater [J]. Fluid machinery, 2010, 38 (11): 81-84.
[27] Nelson Fumo, Pedro Mago, Rogelio Luck. Methodology to estimate building energy consumption using EnergyPlus Benchmark Models[J]. Energy & Buildings, 2010, 42 (12): 2331-2337.
[28] Zhu Mingshan. Exergy analysis of energy system[M]. Beijing: Tsinghua university press, 1988.